Research in Astron. Astrophys. **XXXX** Vol. **X** No. **XX**, 000–000
http://www.raa-journal.org *http://www.iop.org/journals/raa*

***R**esearch in*
***A**stronomy and*
***A**strophysics*

arXiv:1602.06099v3 [astro-ph.HE] 26 Sep 2016

Intensity Distribution Function and Statistical Properties of Fast Radio Bursts

Long-Biao Li[1,2], Yong-Feng Huang[1,2*], Zhi-Bin Zhang[3], Di Li[4,5], Bing Li[1,2,6]

[1] School of Astronomy and Space Science, Nanjing University, Nanjing 210046, China
hyf@nju.edu.cn
[2] Key Laboratory of Modern Astronomy and Astrophysics (Nanjing University), Ministry of Education, Nanjing 210046, China
[3] Department of Physics, College of Sciences, Guizhou University, Guiyang 550025, China
[4] National Astronomical Observatories, Chinese Academy of Sciences, Beijing 100012, China
[5] Key Laboratory for Radio Astronomy, Chinese Academy of Sciences, China
[6] Institute of High Energy Physics, Chinese Academy of Sciences, Beijing 100049, China

Received XXXX ; Accepted XXXX

Abstract Fast Radio Bursts (FRBs) are intense radio flashes from the sky that are characterized by millisecond durations and Jansky-level flux densities. We carried out a statistical analysis on FRBs discovered. Their mean dispersion measure, after subtracting the contribution from the interstellar medium of our Galaxy, is found to be $\sim 660\,\mathrm{pc\,cm^{-3}}$, supporting their being from cosmological origin. Their energy released in radio band spans about two orders of magnitude, with a mean value of $\sim 10^{39}$ ergs. More interestingly, although the FRB study is still in a very early phase, the published collection of FRBs enables us to derive a useful intensity distribution function. For the 16 non-repeating FRBs detected by Parkes telescope and the Green Bank Telescope, the intensity distribution can be described as $dN/dF_{\rm obs} = (4.1 \pm 1.3) \times 10^3\, F_{\rm obs}^{-1.1\pm0.2}\,\mathrm{sky^{-1}\,day^{-1}}$, where $F_{\rm obs}$ is the observed radio fluence in units of Jy ms. Here the power-law index is significantly flatter than the expected value of 2.5 for standard candles distributed homogeneously in a flat Euclidean space. Based on this intensity distribution function, the Five-hundred-meter Aperture Spherical radio Telescope (FAST) will be able to detect about 5 FRBs for every 1000 hours of observation time.

Key words: pulsars: general – stars: neutron – radio continuum: general – intergalactic medium – methods: statistical

1 INTRODUCTION

Fast Radio Bursts (FRBs) are intense radio flashes that seem to occur randomly on the sky. They are characterized by their high brightness ($\geq$ 1 Jy), but with very short durations ($\sim ms$). Until March 2016, 16 non-repeating bursts and one repeat source have been discovered as unexpected outcome of reprocessing pulsar and radio transient surveys (Lorimer et al. 2007; Keane et al. 2012; Thornton et al. 2013; Burke-Spolaor & Bannister 2014; Spitler et al. 2014; Champion et al. 2016; Masui et al. 2015; Petroff et al. 2015a; Ravi, Shannon & Jameson 2015; Keane et al. 2016; Scholz et al. 2016; Spitler et al. 2016). Except for the possible counterpart and host galaxy of FRB 150418 identified in Keane et al. 2016 (but see Vedantham et al. 2016 and Williams & Berger 2016 for different opinions), most previous efforts trying to search for the counterparts of other FRBs have led to a negative result (e.g. Petroff et al.

2015a). Very recently, Spitler et al. (2016) and Scholz et al. (2016) discovered sixteen repeating bursts from the direction of FRB 121102, providing valuable clues to the nature of these enigma events (Dai et al. 2016; Gu et al. 2016). Although FRB 140514 has been detected in almost the same direction as that of FRB 110220, it is considered to be a separate event because of its different dispersion measure (DM) (Petroff et al. 2015b).

The arrival time of a FRB at different wavelength is characterized by a frequency-dependent delay of $\Delta t \propto \nu^{-2}$, and the pulse width is found to scale as $W_{\rm obs} \propto \nu^{-4}$ (Lorimer et al. 2007; Thornton et al. 2013). Both characteristics are consistent with the expectations for radio pulses propagating through a cold, ionized plasma. These facts strengthen the view that FRBs are of astrophysical origin. The dispersion measure, defined as the line-of-sight integral of the free electron number density, is a useful indication of distance. An outstanding feature of FRBs is that their dispersion measures are very large and exceed the contribution from the electrons in our Galaxy by a factor of 10 — 20 in most cases. Lorimer et al. (2007) and Thornton et al. (2013) suggested that the large DM is dominated by the contribution from the ionized intergalactic medium (IGM). FRBs thus seem to occur at cosmological distances. With their large DMs, FRBs may be a powerful probe for studying the IGM and the spatial distribution of free electrons.

The millisecond duration of FRBs suggests that their sources should be compact, and the high radio brightness requires a coherent emission mechanism (Katz 2014a; Luan & Goldreich 2014). Since FRBs' redshifts are estimated to be in the range of $z \sim 0.5$ — 1.3 (Thornton et al. 2013; Champion et al. 2016), the emitted energy at radio wavelengths can be as high as $\sim 10^{39}$ — 10^{40} ergs. Although the physical nature of FRBs is still unclear, some possible mechanisms have been proposed, such as double neutron star mergers (Totani 2013), interaction of planetary companions with the magnetic fields of pulsars (Mottez & Zarka 2014), collapses of hypermassive neutron stars into black holes (Falcke & Rezzolla 2014; Ravi & Lasky 2014; Zhang 2014), magnetar giant flares (Kulkarni et al. 2014; Lyubarsky 2014; Pen & Connor 2015), supergiant pulses from pulsars (Cordes & Wasserman 2016), collisions of asteroids with neutron stars (Geng & Huang 2015; Dai et al. 2016) or the inspiral of double neutron stars (Wang et al. 2016). Keane et al. (2016) suggested that there may actually be more than one class of FRB progenitors.

New FRB detections are being made and much more are expected in the near future. Thornton et al. (2013) have argued that if FRBs happen in the sky isotropically, their actual event rate could be as high as $\sim 10^4\,{\rm sky}^{-1}{\rm day}^{-1}$. Hassall, Keane & Fender (2013) discussed the prospects of detecting FRBs with the next-generation radio telescopes and suggested that the Square Kilometre Array (SKA) could detect about one FRB per hour. Based on the redshifts estimated from the measured DMs, Bera et al. (2016) studied the FRB population and predicted that the upcoming Ooty Wide Field Array[1] can detect FRBs at a rate of ~ 0.01 — 10^3 per day, depending on the power-law index of the assumed distribution function, which could vary from -5 to 5. Note that their predicted detection rate is in a very wide range, which mainly stems from the uncertainty of the FRB luminosity function and their spectral index.

The luminosities depends strongly on the measured redshifts. However, the redshifts of FRBs are not directly measured, but are derived from their DMs. The reliability of these redshifts still needs to be clarified (Katz 2014b; Luan & Goldreich, 2014; Pen & Connor 2015). In this study, we examine the statistical properties of published FRBs, and use the directly measured fluences[2] of FRBs to derive an intensity distribution function. Our distribution function is independent of the redshift measurements. We then use the intensity distribution function to estimate the detection rate of FRBs by the Chinese Five-hundred-meter Aperture Spherical radio Telescope (FAST), the opening ceremony of which is slated for the 25th of September, 2016. Our article is organized as follows. In Section 2, we describe the sample of 16 non-repeating FRBs and present the statistical analyses of their parameters. In Section 3, we derive the intensity distribution function of FRBs. In Section 4, the observational prospects of FRBs with FAST are addressed. Our conclusions and discussion are presented in Section 5.

[1] http://rac.ncra.tifr.res.in/

[2] Note that the usage of the word "fluence" here is different from its common definition and dimension. We follow earlier FRB papers in this study.

Table 1 Key parameters of the 16 non-repeating FRBs. Observational data are mainly taken from http://astronomy.swin.edu.au/pulsar/frbcat/ (Petroff et al. 2016).

FRB	$W_{\rm obs}$ (ms)	$S_{\rm peak}$ (Jy)	$F_{\rm obs}$ (Jy ms)	DM[a] ($\rm pc\,cm^{-3}$)	$DM_{\rm Galaxy}$[a] ($\rm pc\,cm^{-3}$)	$DM_{\rm Excess}$[b] ($\rm pc\,cm^{-3}$)	z[c]	$D_{\rm L}$[c] (Gpc)	E[c] (10^{39} ergs)
(1)	(2)	(3)	(4)	(5)	(6)	(7)	(8)	(9)	(10)
010125	$10.60^{+2.80}_{-2.50}$	$0.54^{+0.11}_{-0.07}$	$5.72^{+2.99}_{-1.92}$	790.3 ± 0.3	110	680.3	0.57	3.35	2.77
010621	$8.00^{+4.00}_{-2.25}$	$0.53^{+0.26}_{-0.09}$	$4.24^{+5.24}_{-1.71}$	748 ± 3	523	223	0.19	0.93	0.12
010724	$20.00^{+0.00}_{-0.00}$	$1.57^{+0.00}_{-0.00}$	31.48	375 ± 3	44.58	330.42	0.28	1.45	2.31
090625	$1.92^{+0.83}_{-0.77}$	$1.14^{+0.42}_{-0.21}$	$2.19^{+2.10}_{-1.12}$	899.55 ± 0.1	31.69	867.86	0.72	4.46	2.42
110220	$5.60^{+0.10}_{-0.10}$	$1.30^{+0.00}_{-0.00}$	$7.28^{+0.13}_{-0.13}$	944.38 ± 0.05	34.77	909.61	0.76	4.77	9.39
110523	$1.73^{+0.17}_{-0.17}$	0.60	1.04	623.30 ± 0.06	43.52	579.78	0.48	2.73	0.22
110626	$1.41^{+1.22}_{-0.45}$	$0.63^{+1.22}_{-0.12}$	$0.89^{+3.98}_{-0.40}$	723.0 ± 0.3	47.76	675.54	0.56	3.28	0.48
110703	$3.90^{+2.24}_{-1.85}$	$0.45^{+0.28}_{-0.10}$	$1.76^{+2.73}_{-1.04}$	1103.6 ± 0.7	32.33	1071.27	0.89	5.80	3.59
120127	$1.21^{+0.64}_{-0.25}$	$0.62^{+0.35}_{-0.10}$	$0.75^{+1.04}_{-0.25}$	553.3 ± 0.3	31.82	521.48	0.43	2.39	0.20
121002	$5.44^{+3.50}_{-1.20}$	$0.43^{+0.33}_{-0.06}$	$2.34^{+4.46}_{-0.77}$	1629.18 ± 0.02	74.27	1554.91	1.30	9.28	14.94
130626	$1.98^{+1.20}_{-0.44}$	$0.74^{+0.49}_{-0.11}$	$1.47^{+2.45}_{-0.50}$	952.4 ± 0.1	66.87	885.53	0.74	4.62	1.75
130628	$0.64^{+0.13}_{-0.13}$	$1.91^{+0.29}_{-0.23}$	$1.22^{+0.47}_{-0.37}$	469.88 ± 0.01	52.58	417.3	0.35	1.87	0.19
130729	$15.61^{+9.98}_{-6.27}$	$0.22^{+0.17}_{-0.05}$	$3.43^{+6.55}_{-1.81}$	861 ± 2	31	830	0.69	4.24	3.35
131104	$2.37^{+0.89}_{-0.45}$	$1.16^{+0.35}_{-0.13}$	$2.75^{+2.17}_{-0.76}$	779 ± 3	71.1	707.9	0.59	3.50	1.72
140514	$2.80^{+3.50}_{-0.70}$	$0.47^{+0.11}_{-0.08}$	$1.32^{+2.34}_{-0.50}$	562.7 ± 0.6	34.9	527.8	0.44	2.46	0.37
150418	$0.80^{+0.30}_{-0.30}$	$2.20^{+0.60}_{-0.30}$	$1.76^{+1.32}_{-0.81}$	776.2 ± 0.5	188.5	587.7	0.49	2.79	0.66

[a] DM and $DM_{\rm Galaxy}$ are the total dispersion measure and the contribution from the local Galaxy, repectively.
[b] The dispersion measure excess, which is defined as $DM - DM_{\rm Galaxy}$.
[c] The redshifts are estimated from the corresponding DM excess. With these redshifts, the luminosity distances ($D_{\rm L}$) and the emitted energies (E) can then be calculated.

2 SAMPLES AND STATISTICAL ANALYSES

We extract the key parameters of 16 non-repeating FRBs detected by Parkes and GBT from the FRB Catalogue of Petroff et al. (2016) [3]. The data are listed in Table 1. At the direction of FRB 121102, additional 16 repeating bursts have been detected (Spitler et al. 2016; Scholz et al. 2016), indicating that all these events may be quite different from other non-repeating FRBs in nature. So we treat these 17 repeating events separately in our following study.

Column 1 of Table 1 provides the FRB names. The observed width or duration of the corresponding radio pulse ($W_{\rm obs}$) is presented in Column 2. Column 3 is the observed peak flux density ($S_{\rm peak}$) of each FRB. Column 4 tabulates the observed fluences ($F_{\rm obs}$) in units of Jy ms, which is calculated as $F_{\rm obs} = S_{\rm peak} \times W_{\rm obs}$. Columns 5, 6, and 7 present the observed DMs of FRBs, the DM contributions from the Galaxy ($DM_{\rm Galaxy}$), and the DM excesses ($DM_{\rm Excess}$), respectively. The DM excess is defined as $DM_{\rm Excess} = DM - DM_{\rm Galaxy}$. The estimated redshift (z) is presented in Column 8, assuming that the density of electrons is a constant for the IGM. The corresponding luminosity distances ($D_{\rm L}$) and the emitted energies (E) are presented in Columns 9 and 10, respectively. Note that there is no reliable estimate on the uncertainties of $DM_{\rm Galaxy}$, therefore, it is not included. Then the uncertainties of $DM_{\rm Excess}$, z, D_L and E are also not available.

[3] http://astronomy.swin.edu.au/pulsar/frbcat/

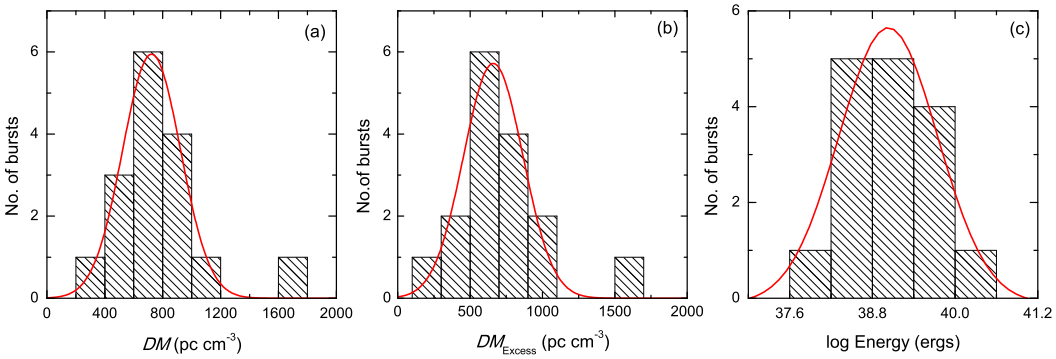

Fig. 1 Distributions of the DM (Panel a), the DM excess (Panel b), and the estimated energy (Panel c). The solid curve in each panel is the best-fit Gaussian function, with the fitting correlation coefficients being 0.90, 0.95 and 0.96 in Panels (a), (b) and (c), respectively.

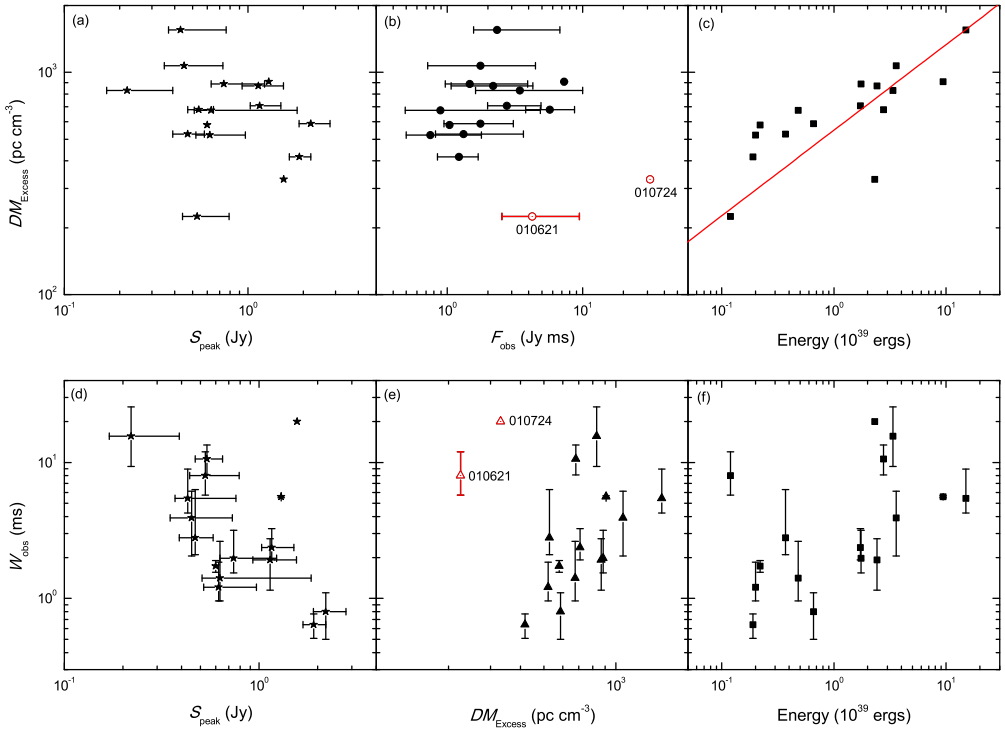

Fig. 2 Panels (a), (b), and (c) illustrate the observed peak flux density ($S_{\rm peak}$), the observed fluence ($F_{\rm obs}$), and the estimated energy (E) against the DM excess ($DM_{\rm Excess}$), respectively. Panels (d), (e) and (f) present $S_{\rm peak}$, $DM_{\rm Excess}$ and E against the observed pulse width ($W_{\rm obs}$), respectively. The best fit line is shown in Panel (c) when the two parameters are clearly correlated.

We first focus on the distribution of the observed DMs of 16 non-repeating FRBs in Table 1. Fig. 1 illustrates the histogram of DMs (Panel a) and DM excesses (Panel b). Both DM and $DM_{\rm Excess}$ roughly follow the normal distribution and can be well fitted with a Gaussian function. The Gaussian function of DM peaks at $723 \pm 45\,{\rm pc\,cm^{-3}}$, while $DM_{\rm Excess}$ peaks at $660 \pm 60\,{\rm pc\,cm^{-3}}$. The standard deviations of these two Gaussian fitting are comparable and of the magnitude of $140\,{\rm pc\,cm^{-3}}$. We see that $DM_{\rm Excess}/DM \sim 90\%$, which supports FRBs' cosmological origin. Panel (c) of Fig. 1 shows that the estimated radio energy approximatively follows a log-normal distribution. The log-normal peak is about 10^{39} ergs, consistent with an earlier estimation by Huang & Geng (2016) when only 10 bursts were available.

In Panels (a), (b) and (c) of Fig. 2, we plot the observed peak flux density, the observed fluence and the estimated radio energy against the DM excess, respectively. Fig. (2a) shows that $S_{\rm peak}$ does not have any clear correlation with $DM_{\rm Excess}$, which is somewhat unexpected since a more distant source usually tends to be dimmer. One possible reason is that $S_{\rm peak}$ depends on the time and frequency resolution of the radio telescope, and another reason may be that the currently observed $DM_{\rm Excess}$ values are still in a relatively narrow range (the largest $DM_{\rm Excess}$ is only $\sim$ 7 times that of the smallest one, and the estimated $D_{\rm L}$ range is a factor of $\sim$ 10). Similarly, Fig. (2b) shows that $F_{\rm obs}$ does not correlate with $DM_{\rm Excess}$. It indicates that the width of FRBs also does not depend on $DM_{\rm Excess}$, which will be further shown in the following figures. In Fig. (2c), we see that the energies shows a strong correlation with $DM_{\rm Excess}$, which is natural since the energy emitted has a square dependence on the distance. In fact, the best fit result of Fig. (2c) is $E \propto DM_{\rm Excess}^{2.59\pm0.39}$, with the correlation coefficient and P-value (rejection possibility) as 0.78 and 1.07×10^{-5}, respectively. It corresponds to a correlation between the energy and the luminosity distance as $E \propto D_{\rm L}^{2.05\pm0.32}$. The power-law index here is roughly consistent with the square relation within a still relatively large error box. Note that the correlation may also be partly caused by the telescope selection effect, because weaker FRB events can be detected only at nearer distances, although they may also happen at far distances. In addition, the sample of FRBs is still limited. It is expected that more FRBs would be detected when radio telescopes with higher sensitivities come into operation in the future.

Fig. (2d) demonstrates the trend for FRBs with brighter peaks ($S_{\rm peak}$) to have narrower width ($W_{\rm obs}$). A similar tendency has been found for giant pulses from some pulsars (e.g. Popov & Stappers 2007; Bhat, Tingay & Knight 2008; Popov et al. 2009; Cordes et al. 2016; Popov & Pshirkov 2016). In the case of FRBs, this correlation can be explained by some possible models. For example, Geng & Huang (2015) argued that FRBs can be produced by the collisions of asteroids with neutron stars. In this scenario, when the asteroid collides with the neutron star with a very small impact parameter, the collision process will finish very quickly and the brightness of the FRB should be high. On the other hand, if the asteroid collides with the neutron star with a slightly larger impact parameter, the collision process will be significantly prolonged and the peak flux of the induced FRB will be correspondingly weaker. It can naturally account for the correlation of $W_{\rm obs}$ and $S_{\rm peak}$ as shown in Fig. (2d). Finally, we see that neither E nor $DM_{\rm Excess}$ correlate with $W_{\rm obs}$ (Figs. (2e) and (2f)). Note that while the observed pulse width is relatively clustered, emitted energies span two orders of magnitude. In Panels (b) and (e), we mark the positions of FRBs 010621 and 010724. These two events seem to be quite different from others. We argue that they may form a distinct group, characterized by a low DM and a large fluence. It suggests the existence of different FRB populations. More events detected in the future will help to clarify such a possibility.

3 INTENSITY DISTRIBUTION FUNCTION

An absolutely scaled luminosity function can help to reveal the nature of FRBs (Bera et al. 2016). Since the redshifts of FRBs have not been independently measured, the derived absolute luminosities and the emitted energies of FRBs are thus controversial (Katz 2014b; Luan & Goldreich 2014; Pen & Connor 2015). On the other hand, the apparent intensity distribution function of astronomical objects can also provide helpful information on their nature. A good example is the study of gamma-ray bursts (GRBs). Before 1997, when the redshifts of GRBs were still unavailable, a deviation from the $-3/2$ power-

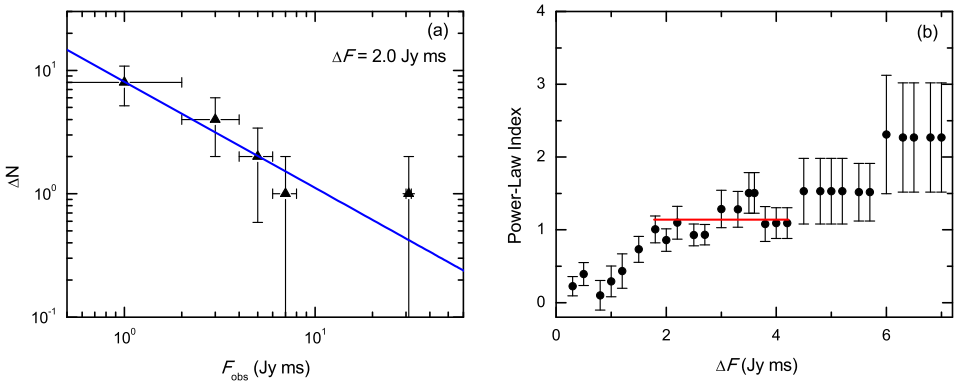

Fig. 3 Intensity distribution functions of 16 non-repeating FRBs listed in Table 1 (Case I). Panel (a) shows an exemplar distribution function for a particular bin width, with the y-axis showing the number of FRBs in each bin. Panel (b) illustrates the best-fitted a values for different bin widths, in which the solid short horizontal line shows the average value of a for a preferable range of ΔF when a is relatively stable.

law in the peak flux distribution of GRBs was noted (Tavani 1998). It was explained as a hint for the cosmological origin of GRBs, which was later confirmed by direct redshift measurements.

Here, we focus on the observed fluence ($F_{\rm obs}$) of FRBs, instead of $S_{\rm peak}$. Seriously affected by scatter and scintillation of IGM, the peak flux density can be relatively unstable. The combination of $W_{\rm obs}$ and $S_{\rm peak}$, i.e. the observed fluence, can then more reliably indicate the fierceness of FRBs. Another reason is that due to the limited time resolving power of our radio receivers, a FRB should last long enough to be recorded so that the duration is also a key factor. In fact, a tentative cumulative distribution vs. the fluence has been drawn by Katz (2016) based on a smaller data set consisting of 10 FRBs. Caleb et al. (2016) has also tried to compose a cumulative $\log N(>F) - \log F$ correlation by using 9 FRBs in the high latitude (Hilat) region of the Parkes survey.

Although the energy distribution of FRBs spans about two orders of magnitude, it is still relatively clustered, which indicates that FRBs can be considered as standard candles to some extent. We can then use the brightness distribution of FRBs to hint their spatial distribution. We assume that the actual number density of FRBs occurring in the whole sky per day at a particular fluence $F_{\rm obs}$ follows a power-law function, i.e. $dN/dF_{\rm obs} = A\,F_{\rm obs}^{-a}$, where A is a constant coefficient in units of events $\rm sky^{-1}\,day^{-1}$ and a is the power-law index. Both A and a need to be determined from observations. We first only consider the 16 non-repeating FRBs in Table 1 as the input data (Case I). We group the 16 FRBs into different fluence bins with a bin width of ΔF, count the number of FRBs in each bin and get the best-fitted power-law function for $dN/dF_{\rm obs}$. In Panel (a) of Fig. 3, we show the best-fitted result when the bin width is taken as $\Delta F = 2.0$ Jy ms. The fitted power-law index is $a = 0.86 \pm 0.15$, with the fitted correlation coefficient being 0.86 and the corresponding P-value being 0.001. Note that the error bars along x-axis simply represent the bin size, and the y-axis error bars are the statistical errors, which are the square root of the number in each bin.

Obviously, since the total number of FRBs is still very limited, the choice of the bin width will seriously affect the fitting result. So, we have tried various bin width ranging from 0.3 Jy ms to 7.0 Jy ms to study the effect. For these different bin widths, the derived power-law indices are illustrated in Panel (b) of Fig. 3. From this panel, we see that when the bin width is very small ($\Delta F \leq 1.8$ Jy ms), the fitted a value depends strongly on the bin width. The reason is that only two or three FRBs are grouped into one bin generally, thus the fluctuation dominates the final result. Meanwhile, when the bin width is too large ($\Delta F > 4.2$ Jy ms), the error bar of the fitted a also becomes larger. In these cases, only two

Table 2 The observable event rate of FRBs in the literature.

$F_{\rm Limit}$ (Jy ms)	$R(>F_{\rm Limit})$ ($\rm sky^{-1}\,day^{-1}$)	Reference	Derived coefficient A ($10^3\,\rm sky^{-1}\,day^{-1}$)
3.0	10^4	Thornton et al. (2013)	5.61 ± 2.04
0.35	3.1×10^4	Spitler et al. (2014)	7.88 ± 6.92
2.0	2.5×10^3	Keane & Petroff (2015)	1.17 ± 0.51
1.8	1.2×10^4	Law et al. (2015)	5.37 ± 2.47
4.0	4.4×10^3	Rane et al. (2016)	2.86 ± 0.90
0.13-5.9	6.0×10^3	Champion et al. (2016)	1.94 ± 1.27

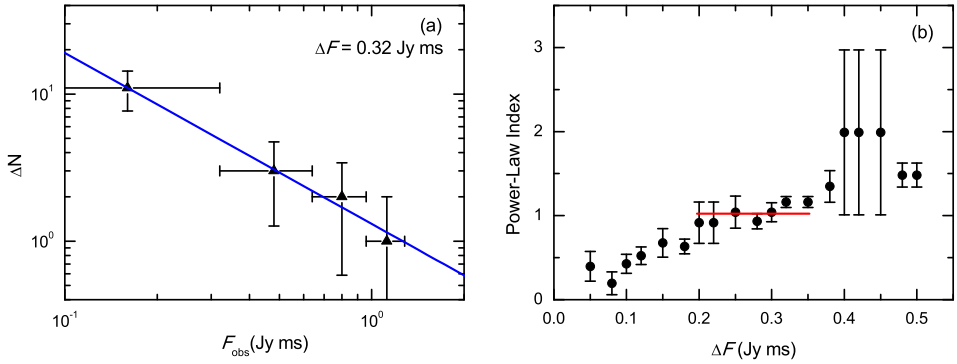

Fig. 4 Intensity distribution functions of the 17 repeating FRBs from the source of FRB 121102 (Case II). Symbols are the same as Fig. 3.

or three bins are left with a non-zero number of FRBs so that the derived a becomes unreliable again. On the contrary, when ΔF is in the range of 1.8 — 4.2 Jy ms, the best-fitted a keeps to be somehow constant and the error box is also small. So we choose such a ΔF range to derive the a parameter. To reduce the effects of fluctuation as far as possible, we add up all the 12 a values derived for ΔF ranging between $1.8\,\rm Jy\,ms \leq \Delta F \leq 4.2\,\rm Jy\,ms$ to get a mean value for a (designated as a_1 for Case I), which finally gives $a_1 = 1.14 \pm 0.20$ (see Fig. (3b)).

Integrating the intensity distribution function, we can derive the FRB event rate above a particular fluence limit in the whole sky per day as

$$R(>F_{\rm Limit}) = A \int_{F_{\rm Limit}}^{F_{\rm max}} F_{\rm obs}^{-a}\, dF_{\rm obs}, \tag{1}$$

where $F_{\rm Limit}$ corresponds to the limiting sensitivity of a radio telescope, $F_{\rm max}$ is the upper limit of the fluence of observed FRBs, which is set as 35 Jy ms in our calculations (the observed maximum fluence is $\sim$ 32 Jy ms at present). A is an unknown coefficient. It still needs to be determined from observations. FRBs were mainly identified from the archival data of several radio surveys. Constraints on the actual event rates of FRBs above a certain fluence limit were also derived in these analyses and were reported in the literature. We sum up these constraints in Table 2. According to Eq. (1), these data can be used to derive the coefficient A by using our best-fit a_1 value. The results are also listed in the last column in Table 2. Combining all these different A values, we finally get a mean value as $A = (4.14 \pm 1.30) \times 10^3\,\rm sky^{-1}\,day^{-1}$. After getting the power-law index a and the constant coefficient

A, we now can write down the full apparent intensity distribution function as,

$$\frac{dN}{dF_{\rm obs}} = (4.14 \pm 1.30) \times 10^3 \, F_{\rm obs}^{-1.14\pm0.20} \, {\rm sky}^{-1} \, {\rm day}^{-1}, \tag{2}$$

where $F_{\rm obs}$ is in units of Jy ms.

In total, 17 repeating FRB events have been detected from the source of FRB 121102. We treat these events as a separate group (Case II) and also study their intensity distribution. Similar fitting processes as for Case I are applied to Case II, the final results are shown in Fig. 4. In Fig. (4a), we show the exemplar fitting result when taking the bin width as $\Delta F = 0.32$ Jy ms. The best-fitted power-law index is 1.16 ± 0.06, with the correlation coefficient and P-value being 0.99 and 0.001, respectively. Similar to Fig. (3b), Fig. (4b) shows the derived a values for different bin widths. The most probable mean value of a (designated as a_2 for Case II) is calculated for ΔF ranging between 0.2 Jy ms and 0.35 Jy ms, which is $a_2 = 1.03 \pm 0.16$. Note that although a_1 and a_2 do not differ from each other markedly, there are actually significant differences between the overall characteristics of non-repeating FRBs and repeating FRBs. For example, the most obvious difference is that the repeating FRBs are generally weaker, indicating that they are mainly at the weak end of the fluence distribution.

4 PROSPECTS FOR FAST

FAST (Nan et al. 2011; Li, Nan & Pan 2013), an ambitious Chinese mega-science project, is currently being built in Guizhou province in southwestern China. With a geometrical diameter of 500 meters and an effective diameter of ~ 300 meters at any particular moment, it will be the largest single-dish radio telescope in the world when it comes into operation in September of 2016. FAST's receivers will cover both low frequency (70-500 MHz) and middle frequency (0.5-3 GHz) bands. We here consider the prospect of detecting FRBs with FAST by using the derived intensity distribution function. Our calculations are done at the L band (1400 MHz) of FAST, which is the central observational frequency for most detected FRBs.

The sensitivity or the limiting flux density ($S_{\rm limit}$) of a radio telescope can be estimated as (Zhang et al. 2015),

$$\begin{aligned} S_{\rm limit} \simeq (12\mu{\rm Jy})(\frac{0.77 \times 10^3 {\rm m}^2/{\rm K}}{A_{\rm e}/T_{\rm sys}})(\frac{S/N}{3})(\frac{1{\rm hour}}{\Delta\tau})^{1/2} \\ (\frac{100{\rm MHz}}{\Delta\nu})^{1/2}, \end{aligned} \tag{3}$$

where $T_{\rm sys}$ is the system temperature, $\Delta\tau$ is the integration time, $\Delta\nu$ is the bandwidth, ${\rm S/N}$ is the signal-to-noise ratio which is usually taken as 10 for a credible detection of a FRB (Champion et al. 2016), $A_{\rm e}$ is the effective area and it equals to $\eta_A \, \pi \, (d/2)^2$, with η_A being the aperture efficiency and d being the illuminated diameter. FAST has a system temperature of $T_{\rm sys} \sim 25K$ at 1400 MHz. For other parameters of FAST, we take $d = 300\,{\rm m}$, $\eta_A = 0.65$ (Zhang et al. 2015), $\Delta\nu = 300$ MHz, $\Delta\tau = 3$ ms (Law et al. 2015). The limiting fluence of FAST is then calculated to be $F_{\rm Limit} = S_{\rm limit} \times \Delta\tau = 0.03$ Jy ms. Note that from Equations (1) and (2), the actual FRB event rate above the fluence limit of 0.03 Jy ms is $(3.03 \pm 1.56) \times 10^4 \, {\rm sky}^{-1} \, {\rm day}^{-1}$.

The beam size of a radio telescope is $\Omega \sim \pi\theta^2$, where $\theta \sim 1.22(\lambda/d)$ is the half opening angle of the beam. For FAST, the beam size is $\Omega \sim 0.008 \, {\rm deg}^2$ at 1400 MHz. FAST's reciver has 19 beams in L band, and the corresponding total instantaneous field-of-view (FoV) is $0.15 \, {\rm deg}^2$. Considering Eq. (2) and all these parameters, we can get the daily detection rate of FRBs by FAST as,

$$\begin{aligned} R_{\rm FAST} &\sim (3.03 \pm 1.56) \times 10^4 \times \frac{0.15 \, {\rm deg}^2}{41253 \, {\rm deg}^2} \, {\rm day}^{-1} \\ &= 0.11 \pm 0.06 \, {\rm day}^{-1}. \end{aligned} \tag{4}$$

For a 1000 hours of observation time, this corresponds to $\sim 5 \pm 2$ detections.

5 DISCUSSION AND CONCLUSIONS

In this study, we analysed statistically the key parameters of the 16 non-repeating FRBs detected by Parkes and GBT. The observed DM spans a range of 375 — 1629 $\mathrm{pc\,cm^{-3}}$ and peaks at $\sim 723\,\mathrm{pc\,cm^{-3}}$, while the DM excess peaks at $\sim 660\,\mathrm{pc\,cm^{-3}}$ and typically accounts for $\sim 90\%$ of the total DM. The emitted radio energy spans about two orders of magnitude, with the mean energy being about 10^{39} ergs. While most of the parameters do not correlate with each other, a burst with stronger $S_{\rm peak}$ tends to have shorter duration. Meanwhile, a clear correlation between the radio energy released and the DM excess has been found to be $E \propto DM_{\rm Excess}^{2.59\pm0.39}$ (Fig. 2c), which may reflect the square dependence of the emitted energy on the distance. But note that the observational selection effect may also play a role in the statistics. From these statistical analyses, we found that FRBs 010621 and 010724 are quite different from others and they may form a distinct group.

Using the observed fluence as an indication for the strength of FRBs and combining the constraints on the event rate of FRBs from various observational surveys, we derived an apparent intensity distribution function for the 16 non-repeating FRBs as $dN/dF_{\rm obs} = (4.14 \pm 1.30) \times 10^3\, F_{\rm obs}^{-1.14\pm0.20}\,\mathrm{sky^{-1}\,day^{-1}}$. For FRB 121102 and its repeating bursts, the corresponding power-law index is derived to be $a_2 = 1.03 \pm 0.16$. Based on the intensity distribution function, we were able to estimate the detection rate of FRBs by China's coming FAST telescope. With a sensitivity of 0.03 Jy ms and a total instantaneous FoV of 0.15 deg^2 (19 beams), FAST will be able to detect roughly 1 FRB for every 10 days of observations, or about 5 events for every 1000 hours.

A few authors have studied the cumulative distribution function of FRBs (Bera et al. 2016; Caleb et al. 2016; Katz 2016; Wang & Yu 2016), which is usually assumed to be a power-law function of $N_{>F_{\rm obs}} \propto F_{\rm obs}^{-\alpha}$. For standard candles distributed homogeneously in a flat Euclidean space, the value of α should be 3/2 (Thornton et al. 2013). Oppermann, Connor & Pen (2016) has argued that the range of α may be $0.9 \leq \alpha \leq 1.8$, Caleb et al. (2016) has derived $\alpha = 0.9$ for a small sample of 9 Hilat FRBs, while Wang & Yu (2016) considered α as 0.78 for FRB 121102 and its 16 repeating bursts. Note that the relation between the cumulative index α and our intensity distribution index a is $\alpha = a - 1$. So, our derived index of $a = 1.14 \pm 0.20$ will correspond to $\alpha = 0.14 \pm 0.20$. It is significantly smaller than Caleb et al.'s value. The difference could be caused by different sample capacity. We have 16 non-repeating FRBs in our sample. It strongly points toward a deficiency of the dimmest FRBs, which has also been indicated in earlier studies (Bera et al. 2016; Caleb et al. 2016; Lyutikov, Burzawa & Popov 2016). There are a few factors that could lead to such a deviation. First, the total number of currently observed FRBs is still very limited. It can result in a large fluctuation in the measured power-law index. In fact, Caleb et al. (2016) have estimated that at lease ~ 50 FRBs are needed to extract conclusive information on the physical nature of FRBs. Second, FRBs are not ideal standard candles. But as long as the characteristics of FRBs does not evolve systematically with the distance, the index will not be affected too much. A wider brightness range will only result in a larger error box for α, which can still be reduced by increasing the FRB samples. Third, FRBs may not be homogeneous sources, the co-moving density or their brightness may evolve in space. For example, the co-moving FRB density may be smaller when the distance increases, or farther FRBs may not be as fierce as those nearer to us. Fourth, the space may not be a flat Euclidean space, such as for a curved Λ-CDM cosmology. In this case, the deviation of α from 3/2 can be used as a probe for the cosmology (Caleb et al. 2016). Finally, it should also be noted that the apparent deficiency of the dimmest FRBs could also be due to the selection effect. Much weaker FRB events may actually have happened in the sky, but we were not able to record them or find them due to current technical limitations. To make clear which of the above factors has led to the smaller α, more new FRB samples would be necessary in the future.

As addressed above, the apparent intensity distribution function derived here is still a preliminary result. We need much more samples to determine the power-law index more accurately. With an enormous effective area for collecting radio emissions, the Chinese FAST telescope is very suitable for FRB observations. It may be able to increase the FRB samples at a rate of ~ 10 events per year (assuming an effective observation time of 2000 hours). More importantly, FAST can operate in a very wide frequency

range and can hopefully provide detailed spectrum information for FRBs. It is expected to be a powerful tool in the field.

At present, whether FRBs are beamed or not is still an unclear but important problem. If FRBs are highly collimated, the actual energy released will be much smaller than the currently estimated energy base on an assumed solid angle of $\sim 1\,\mathrm{sr}$ (Huang & Geng 2016). The emission mechanisms of FRBs will then involve complex jet effects (Borra 2013). Studying the jet effects of FRBs will be an important task and it will help us understand the explosion mechanisms of FRBs. When more FRBs are observed and localized, we may be able to get useful information on the beaming effects from direct observations.

Acknowledgements This study was supported by the China Ministry of Science and Technology under State Key Development Program for Basic Research (973 program, Grant Nos. 2014CB845800, 2012CB821802), the National Natural Science Foundation of China (Grant Nos. 11473012, U1431126, 11263002) and the Strategic Priority Research Program (Grant No. XDB09010302).

References

Bera, A., Bhattacharyya, S., Bharadwaj, S., Bhat, N. D. R., & Chengalur, J. N. 2016, MNRAS, 457, 2530
Bhat, N. D. R., Tingay, S. J., & Knight, H. S. 2008, ApJ, 676, 1200
Borra, E. F., 2013, ApJ, 774, 142
Burke-Spolaor, S., & Bannister, K. W. 2014, ApJ, 792, 19
Caleb, M., Flynn, C., Bailes, M., et al. 2016, MNRAS, 458, 708
Champion, D. J., Petroff, E., Kramer, M., et al. 2016, MNRAS, 460, L30
Cordes, J. M., & Wasserman, I. 2016, MNRAS, 457, 232
Cordes, J. M., Wharton, R. S., Spitler, L. G., Chatterjee, S., & Wasserman, I. 2016, ApJ, submitted (arXiv:1605.05890)
Dai, Z. G., Wang, J. S., Wu, X. F., & Huang, Y. F. 2016, ApJ, accepted (arXiv:1603.08207)
Falcke, H., & Rezzolla, L. 2014, A&A, 562, A137
Geng, J. J., & Huang, Y. F. 2015, ApJ, 809, 24
Gu, W. M., Dong, Y. Z., Liu, T., Ma, R., & Wang, J. F. 2016, ApJL, 823, L28
Hassall, T. E., Keane, E. F., & Fender, R. P. 2013, MNRAS, 436, 371
Huang, Y. F., & Geng, J. J. 2016, in Proceedings of "Frontiers in Radio Astronomy and FAST Early Sciences Symposium 2015 (FRA 2015)", conference hold in Guiyang, China in July 2015, Astronomical Society of the Pacific, 502, 1
Katz, J. I. 2014a, Phys. Rev. D, 89, 103009
Katz, J. I. 2014b, preprint (arXiv:1409.5766)
Katz, J. I. 2016, ApJ, 818, 19
Keane, E. F., & Petroff, E. 2015, MNRAS, 447, 2852
Keane, E. F., Stappers, B. W., Kramer, M., & Lyne, A. G. 2012, MNRAS, 425, L71
Keane, E. F., Johnston, S., Bhandari, S., et al. 2016, Nature, 530, 453
Kulkarni, S. R., Ofek, E. O., Neill, J. D., Zheng, Z., & Juric, M. 2014, ApJ, 797, 70
Law, C. J., Bower, G. C., Burke-Spolaor, S., et al. 2015, ApJ, 807, 16
Li, D., Nan, R. D., & Pan, Z. C. 2013, in van Leeuwen V., ed, Proc. IAU Symp. 291, Neutron Stars and Pulsars: Challenges and Opportunities After 80 Years. Cambridge Univ. Press, Cambridge, p. 325
Lorimer, D. R., Bailes, M., McLaughlin, M. A., Narkevic, D. J., & Crawford, F. 2007, Science, 318, 777
Luan, J., & Goldreich, P. 2014, ApJ, 785, L26
Lyubarsky, Y. 2014, MNRAS, 442, L9
Lyutikov, M., Burzawa, L., & Popov, S. B., 2016, MNRAS, 462, 941
Mottez, F., & Zarka, P. 2014, A&A, 569, A86
Masui, K., Lin, H., Sievers, J., et al. 2015, Nature, 528, 523
Nan, R. D., Li, D., Jin, C. J., et al. 2011, Int. J. Mod. Phys. D, 20, 989
Oppermann, N., Connor, L., & Pen, U.-L. 2016, MNRAS, 461, 9840

Pen, U.-L., & Connor, L. 2015, ApJ, 807, 179
Petroff, E., Bailes, M., Barr, E. D., et al. 2015a, MNRAS, 447, 246
Petroff, E., Johnston, S., Keane, E. F., et al. 2015b, MNRAS, 454, 457
Petroff, E., Barr, E. D., Jameson, A., et al. 2016, PASA, 33, 45
Popov, M. V., & Stappers, B. 2007, A&A, 470, 1003
Popov, M., Soglasnov, V., Kondratiev, V., et al. 2009, PASJ, 61, 1197
Popov, M., & Pshirkov, M. S. 2016, MNRAS, 462, L16
Rane, A., Lorimer, D. R., Bates, S. D., et al. 2016, MNRAS, 455, 2207
Ravi, V., & Lasky, P. D. 2014, MNRAS, 441, 2433
Ravi, V., Shannon, R. M., & Jameson, A. 2015, ApJL, 799, L5
Scholz, P., Spitler, L. G., Hessels, J. W. T., et al. 2016, ApJ, submitted (arXiv:1603.08880)
Spitler, L. G., Cordes, J. M., Hessels, J. W. T., et al. 2014, ApJ, 790, 101
Spitler, L. G., Scholz, P., Hessels, J. W. T., et al. 2016, Nature, 531, 202
Thornton, D., Stappers, B., Bailes, M., et al. 2013, Science, 341, 53
Totani T., 2013, PASJ, 65, L12
Vedantham, H. K., Ravi, V., Mooley, K., et al. 2016, ApJL, 824, L9
Wang, F. Y., & Yu, H. 2016, preprint (arXiv:1604.08676)
Wang, J. S. Yang, Y. P., Wu, X. F., Dai, Z. G., & Wang, F. Y. 2016, ApJL, 822, L7
Williams, P. K. G., & Berger, E. 2016, ApJL, 821, L22
Zhang, B. 2014, ApJL, 780, L21
Zhang, Z. B., Kong, S. W., Huang, Y. F., Li, D., & Li, L. B. 2015, RAA, 15, 237